N71-16472

AED R-3692F
Issued: January 10, 1971

NASA CR-116220

Sixth Quarterly Report
Study to Determine and Improve Design for Lithium-Doped Solar Cells

Prepared for
Jet Propulsion Laboratory
California Institute of Technology
Pasadena, California
In fulfillment of
Contract No. 952555
October 1 to December 31, 1970

Prepared by
T. Faith, G. Brucker, and
A. Holmes-Siedle

CASE FILE
COPY

RCA | Government and Commercial Systems
Astro Electronics Division | Princeton, New Jersey

AED R-3692F
Issued: January 10, 1971

Sixth Quarterly Report
Study to Determine and Improve Design for Lithium-Doped Solar Cells

Prepared for
Jet Propulsion Laboratory
California Institute of Technology
Pasadena, California
In fulfillment of
Contract No. 952555
October 1 to December 31, 1970

Prepared by
T. Faith, G. Brucker, and
A. Holmes-Siedle

RCA | Government and Commercial Systems
Astro Electronics Division | Princeton, New Jersey

PREFACE

This is the Sixth Quarterly Report on a program for a "Study to Determine and Improve Design for Lithium-Doped Solar Cells." This report was prepared under Contract No. 952555 for Jet Propulsion Laboratory, Pasadena, California, by the Astro-Electronics Division of RCA, Princeton, New Jersey. The preparation of this report is a contractual requirement covering the period from October 1 to December 31, 1970. The work reported here was conducted by the Radiation Effects group, Manager, Dr. A.G. Holmes-Siedle, of AED, which is located at the RCA Space Center. The Project Supervisor is Dr. A.G. Holmes-Siedle and the Project Scientist is Dr. G.J. Brucker. The Technical Monitor of the program is Mr. Paul Berman of the Solar Power group, Jet Propulsion Laboratory.

ABSTRACT

This is the Sixth Quarterly Report on a program to study and analyze the action of lithium in producing a recovery or spontaneous annealing of radiation damage in bulk silicon and silicon solar cells. This program has technical continuity with the work performed by AED of RCA for JPL on Contract No. 952249. The goal of this effort is to understand the damage and recovery mechanisms so that an optimum set of solar-cell design rules can be specified

The test vehicles used for this work are (1) a group of solar cells supplied by JPL, and (2) silicon bars in the "Hall-bar" configuration. The source of particle irradiation being used is a 1-MeV electron beam produced by the RCA Laboratories Van de Graaff generator. As called for in the contract, the Hall measurements terminated with the completion of the Fourth Quarterly Report. The solar cell testing will continue for the duration of the contract.

In the present contract period, photovoltaic recovery measurements have continued on cells from lots H3A, H7A, and C11. Cells irradiated to fluences ranging from 1×10^{14} to 3.6×10^{14} e/cm^2 have reached peak cell recovery with maximum powers (under 140 mW/cm^2 tungsten illumination) ranging up to 20 percent above those of simultaneously irradiated 10 ohm-cm commercial n/p cells. During these experiments it was observed that the recovered value of open-circuit voltage, V_{oc}, increases monotonically with lithium density gradient, dN_L/dw. In H3A cells ($\phi = 3.6 \times 10^{14}$ e/cm^2), recovered values of V_{oc} ranged from 500 to 560 mV over a lithium gradient range of 4×10^{17} to 1.3×10^{19} cm^{-4}.

Short-circuit current recovery experiments on quartz-crucible cells irradiated to a fluence of 1×10^{14} e/cm^2 showed that the time to half recovery, θ, can be described by the approximate relation

$$\theta dN_L/dw \approx 2.4 \times 10^{20} \text{ days/cm}^4$$

This result when combined with a previously obtained result on oxygen-lean cells yielded

$$\theta D_L \, dN_L/dw \approx 5 \times 10^8 \text{ cm}^{-2},$$

where D_L is the lithium diffusion constant, which applies to both oxygen-rich and oxygen-lean cells irradiated to this fluence.

Capacitance measurements on several hundred lithium cells have been used to establish a relationship between the lithium density at the edge of the depletion region, N_{LO}, and dN_L/dw;

for oxygen-lean cells:

$$N_{LO} \approx 1.2 \times 10^3 \left(\frac{dN_L}{dw}\right)^{0.62}$$

for oxygen-rich cells

$$N_{LO} \approx 1.1 \times 10^6 \left(\frac{dN_L}{dw}\right)^{0.46} .$$

These relationships reduce the number of capacitance measurements required to obtain the value of dN_L/dw, which is used in the prediction of cell behavior. Capacitance measurements have also traced the probable cause for previously reported V_{OC} degradation in C4 cells to a levelling off of the lithium density near the junction, i.e., to a negative d^2N_L/dw^2.

TABLE OF CONTENTS

LIST OF ILLUSTRATIONS

TABLE

SECTION I

INTRODUCTION

A. GENERAL

This contract effort represents an experimental investigation of the physical properties of lithium-containing p-on-n solar cells and bulk silicon samples, and of the processes which occur in these devices and samples before and after irradiation. The program objectives are to develop and reduce-to-practice analytical techniques to characterize the radiation resistance of lithium-doped solar cells and its dependence on the materials and processes used to fabricate them. On the basis of these and other data, AED will determine and recommend an improved design of lithium-doped solar cells for space use. A previous RCA program (Contract No. 952249) performed for JPL provided the groundwork for this effort. Unless otherwise mentioned, the source of all irradiations was the 1-MeV electron beam of the RCA Laboratories Van de Graaff generator.

B. TECHNICAL APPROACH

The approach to the objectives is based on the irradiation and measurement of the electrical properties of bulk-silicon samples and government-furnished (GFE) solar cells. Experiments on bulk samples have included Hall and resistivity measurements taken as a function of: (1) bombardment temperature, (2) resistivity, (3) fluence, (4) oxygen concentration, and (5) annealing time at room temperature. Diffusion length and photovoltaic measurements on solar cells are being made as a function of the same five parameters as for bulk samples. In addition, capacitance are made on selected cells. Stability studies are being conducted on solar cells, which have been irradiated and observed for long periods of time. Based on these results, a set of preliminary design rules and specifications have been determined, and solar cells are being procured by JPL in accordance with these rules. As a check of the validity of the design rules, tests will be conducted on this group of cells and a set of modified design rules will be derived.

C. SUMMARY OF PREVIOUS WORK

Some overall conclusions of previous reporting periods were as follows: the low-temperature measurements of Hall bars and of solar cells proved very successful and provided some fruitful insights into the processes occurring in

lithium-containing silicon. Correlation of lifetime damage constant K_τ with the carrier-removal rates, measured as a function of bombardment temperature ($\approx 80°$ K to 200° K), was experimentally demonstrated.

Hall and resistivity measurements on samples of float-zone silicon doped with lithium to concentrations of 2 to 5×10^{14} Li/cm^3 and bombarded by electrons indicated the production of a defect located in the forbidden energy gap at an energy of 0.12 eV below the conduction band. This defect was produced at bombardment temperatures ranging from 78° K to 200° K. Annealing of these samples at a temperature of 100° C did not remove the defect completely, although the concentration was reduced. These lightly doped samples exhibited annealing properties and carrier-removal rates ($\Delta n/\Delta\phi = 0.1$ cm^{-1} at $T_B = 100°$K to 200° K) which are similar to those of heavily doped (2×10^{16} Li/cm^3) quartz-crucible Hall bar samples. The results of the Hall bar experiments suggested that the ratio of oxygen to lithium concentration is an important parameter in determining the annealing properties in lithium-doped silicon. These properties include the stability of both the lithium neutralized and unannealed defect centers, and also the carrier-removal rate for high bombardment temperatures ($T_B = 100°$K to 200° K). Defects located at an energy of $\approx E_C - 0.18$ eV and $\approx E_C - 0.13$ eV were measured in quartz-crucible silicon of moderate resistivity (2×10^{15} Li/cm^3) bombarded by electrons at temperatures from 78° K to 200° K. Both of these defects anneal at room temperature by the interaction of lithium with the defects. These defects would only influence the electrical characteristics of solar cells operating at room temperature if the lithium concentration in the cell was adjusted so as to locate the Fermi level within 2 kT of the defect energy level.

The rate of carrier-removal ($\Delta n/\Delta\phi$ cm^{-1}) SAT appears to increase with decreasing lithium concentration. This suggests that the lithium combined with oxygen so as to limit the oxygen concentration available for A-center formation and the introduction rate of the LiOV center is lower than the A-center introduction rate.

Annealing results obtained on the quartz-crucible Hall bars suggest that several competing processes take place during the post-bombardment period. The short-term experimental results cannot be explained on the basis of a single or a double lithium ion neutralizing a defect. Over a long period of time following bombardment, the results can be explained as due to a multiple complexing by many lithium ions at a defect center so as to produce an uncharged complex.

Cold finger experiments were performed on oxygen-lean cells and on quartz-crucible cells with a wide range of lithium density gradients. Bombardment temperature, T_B, dependence of lifetime damage constant, K_τ, was measured. Both types of cells displayed a saturation of K_τ at high T_B and a decrease at lower temperatures in agreement with results previously obtained from carrier removal experiments on Hall samples. K_τ saturated at $T_B = 100°$K to 120° K.

The lifetime damage constant for $T > 120°K$ is a factor of ≈ 5 higher in oxygen-lean lithium cells than in crucible (Li) cells and is not strongly dependent on lithium density, changing less than a factor of 2 over a lithium gradient range of ≈ 30.

Recovery rate measurements versus annealing temperature showed the activation energy for recovery in several groups of crucible cells to be ≈ 1.1 eV which is the activation energy for lithium diffusion in crucible-grown silicon, and that for several groups of oxygen-lean cells to be ≈ 0.65 eV, the activation energy for lithium diffusion in silicon with low-oxygen content.

Diffusion constant measurements made on quartz-crucible cells show an activation energy of 1.03 eV indicative of dissociation of LiO^+ and diffusion of Li^+.

Performance tests on the solar cells showed that most of the lithium cells from recent shipments had initial powers greater than the commercial n/p cells. The pre-irradiation lithium donor density gradient, dN_L/dw, provides a good index of the lithium density distribution near the junction and of the dynamic behavior of cell.

Long-term stability tests at room temperature on lithium-containing crucible-grown cells continued to show these cells to be stable. Most of the crucible cells which have completed their recovery cycles were competitive in power with commercial 10 ohm-cm n/p cells irradiated to the same fluence. For a fluence of 3×10^{14} e/cm^2, the time-to-half-recovery, θ, of these cells was related to the lithium density gradient dN_L/dw, through $\theta\, dN_L/dw = 6.5 \pm 2.5 \times 10^{20}$ days/cm^4 for $10^{18} \leqslant dN_L/dw \leqslant 5 \times 10^{19}$ cm^{-4}. Oxygen-lean cells with heavy lithium doping ($dN_L/dw \gtrsim 10^{19}$ cm^{-4}) have suffered some form of instability, either post-recovery redegradation or instability independent of irradiation. The post-recovery short-circuit current redegradation was the most common instability. However, cells which suffered this instability did stabilize after a ≈ 100 day redegradation period. A radiation independent open-circuit voltage instability was suffered by cells of lot C4. This loss, which is due to carrier loss in the base region has occurred continuously over ≈ 500 days.

SECTION II

PERFORMANCE OF JPL-FURNISHED CELLS

A. GENERAL

The principal effort during this reporting period has been directed toward the study of the physical properties of the lithium cell and how these properties influence cell performance and stability. In addition, photovoltaic recovery tests were performed on lithium cells from recent shipments which were irradiated in the previous reporting period. The experimental data obtained during this period consisted mainly of reverse bias capacitance measurements from which the lithium density profile was calculated (Ref. 1) and of measurements of cell photovoltaic characteristic under 140 mW/cm^2 tungsten illumination.

B. LITHIUM CELL PERFORMANCE

Lithium cell recovery was monitored on several groups of cells out to the peak recovered value. These cell groups came from the high performance cell lots received during the present contract year. Their initial performance was reported on in the previous Quarterly Report (Ref. 2). Table I lists the cell groups, the number of cells in each group, the fluence they experienced and the average recovered power for each group together with the recovered power for 10 ohm-cm commercial n/p cells simultaneously irradiated. The numbers indicate higher recovered power in each of the lithium cell groups than in the corresponding n/p cells, the advantage ranging up to 13 percent in the case of the C11C(1) cells with one of the C11C cells, at 30 mW being 20 percent above the n/p cell.

C. CELL RECOVERY AND LITHIUM GRADIENT

1. Extent of Recovery

The values listed in Table I represent the averages over the entire cell group. However some of the groups, i.e., the C11 groups and H3A(2), cover a wide range of lithium density gradients (dN_L/dw) and, consequently, as previously shown, (Ref. 2 and 3) have a wide range of recovery speeds. Recent work has shown that the recovered power after exposure to moderate ($\gtrsim 3 \times 10^{14}$ e/cm^2) fluences also indicates a systematic trend versus lithium density gradient. This is illustrated in Figure 1 in which recovered maximum power after a fluence of 3×10^{14} e/cm^2 is plotted for each cell in groups C11A(1) and C11D(1)

TABLE I. RECOVERED MAXIMUM POWER OF LITHIUM CELL GROUPS COMPARED WITH COMMERCIAL 10 ohm-cm n/p CELLS (POWERS AVERAGED OVER EACH CELL GROUP)

Cell Group	No. of Cells	Type	ϕ(e/cm^2)	Recovered Power (mW)	
				P_{max}(Li)	P_{max}(n/p)
C11B(1)	7	QC*	1×10^{14}	25.8	24.8
C11C(1)	8	LOPEX	1×10^{14}	28.1	24.8
C11A(1)	4	QC*	3×10^{14}	23.4	22.1
C11D(1)	3	QC*	3×10^{14}	24.9	22.1
H7A(1)	3	FZ	3×10^{14}	24.6	22.1
H3A(2)	8	QC*	3.6×10^{14}	22.7	20.6

* QC cells stored at 60° C or 80° C to speed recovery rate.

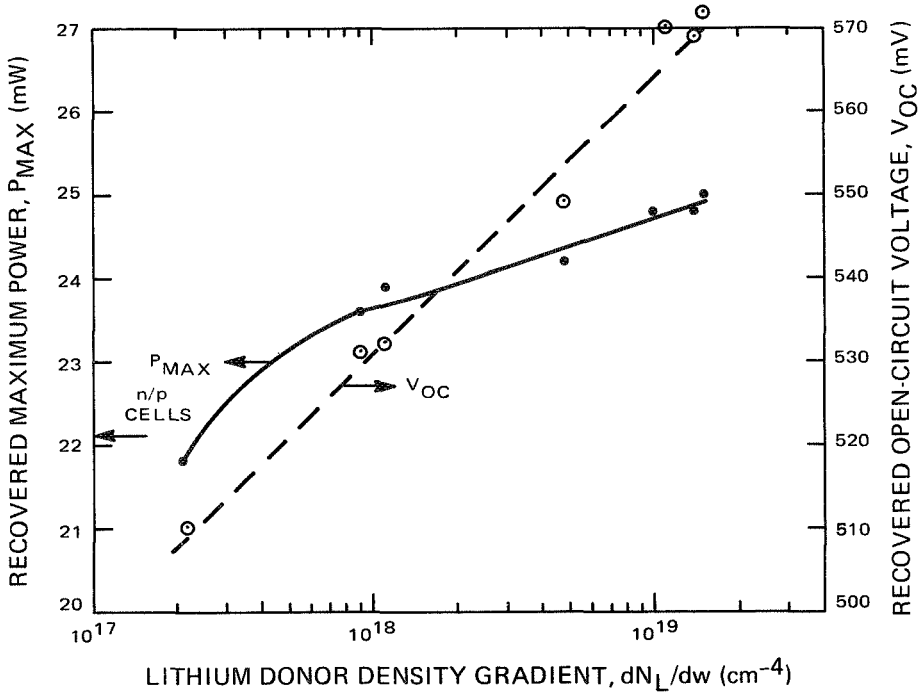

Figure 1. Recovered Maximum Power and Open-Circuit Voltage vs Lithium Density Gradient, C11A and C11D Cells After Recovery from $\phi = 3 \times 10^{14}$ e/cm^2

versus lithium density gradient. The recovered power level clearly increases with lithium density gradient, the main reason for this increase being the dependency of the recovered value of open-circuit voltage (V_{OC}) on the lithium density gradient, which is also plotted in Figure 1. The recovered V_{OC} values span a range of 62 mV (510 to 572 mV). This range is much larger than either the pre-irradiation range of 30 mV (590 to 620 mV) or the immediate post-irradiation range of 23 mV (502 to 525 mV). A similar situation exists for group H3A(2) where the lithium gradient ranges from 4×10^{17} to 1.3×10^{19} cm^{-4}. The pre-irradiation V_{OC}'s covered a 15-mV range (579 to 594 mV) while the post-recovery values ($\phi = 3.6 \times 10^{14}$ e/cm^2) ranged over 60 mV, from 500 to 560 mV, increasing monotonically with lithium gradient. Experiments which extend these studies of lithium-gradient dependencies to higher fluences are now being conducted.

2. Speed of Recovery

In the previous quarterly report (Ref. 2) results of recovery experiments on C11C (Lopex) cells were given in which the recovery speed was shown to vary linearly with lithium density gradient. During the present reporting period similar experiments were performed on C11B (quartz-crucible) cells. Since the room-temperature recovery rate for crucible cells is very slow, the C11B cells were stored at 60° C. The recovery times at 60° C were converted to equivalent room-temperature times through the previously observed (Ref. 4) activation energy for crucible cell recovery, 1.1 eV. The results are shown in Figure 2 which also shows the results for C11C cells. Time to half recovery, θ, is plotted against lithium density gradient, dN_L/dw. The time, θ, is defined by

$$\frac{I(\theta) - I(o)}{I(R) - I(o)} = 0.5, \tag{1}$$

where I(o) and I(R) are the short-circuit currents immediately after irradiation and at completion of recovery, respectively, and $I(\theta)$ is the short-circuit current at time θ.

The results indicate that for crucible cells, as well as Lopex cells, the speed of recovery varies approximately linearly with dN_L/dw. From Figure 2 the appropriate equation for the curcible cells is

$$\theta dN_L/dw \approx 2.4 \times 10^{20} \text{ days/cm}^4, \tag{2}$$

and that for the Lopex (oxygen-lean) cells is

$$\theta dN_L/dw \approx 3.2 \times 10^{17} \text{ days/cm}^4. \tag{3}$$

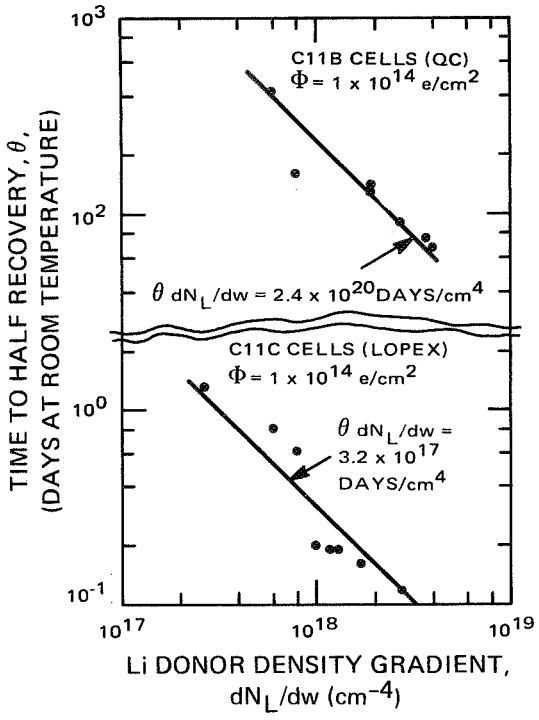

Figure 2. Time to Half Recovery vs Lithium Density Gradient for Seven Oxygen-Rich and Eight Oxygen-Lean Lithium Cells

The ratio of these two products is $\approx 10^3$ which is the ratio (Ref. 5) of the lithium diffusion constants (at room temperature) in oxygen-lean and oxygen-rich silicon ($D_L = 2 \times 10^{-14}$ cm^2/sec in oxygen-lean silicon). Using these facts, Equations (2) and (13) can be combined to yield:

$$\theta D_L \, dN_L/dw \approx 5 \times 10^8 \text{ cm}^{-2}, \qquad (4)$$

which applies to both oxygen-rich and oxygen-lean cells.

Equation (4) applies only to the fluence to which the C11B and C11C cells were irradiated, i.e., 1×10^{14} e/cm^2. Previous results (Ref. 3) have yielded a higher product of $\theta dN_L/dw \approx 6 \times 10^{20}$ days/cm^4 for crucible cells irradiated to the higher fluence of 3×10^{14} e/cm^2. In addition, an equation of the form of Equation (4) can hold only for fluences low enough that the density of defects is small compared to the lithium density. If this is not the case the effective lithium gradient after irradiation will not approximate the gradient measured, i.e., that prior to irradiation. Cells are now being gathered for experiments which will expand the range of gradients covered and hopefully uncover a specific fluence dependence to insert into, and thus expand the range of validity of Equation (4).

D. DAMAGE FACTORS AND LITHIUM GRADIENT

Although carrier removal experiments on lithium-doped silicon Hall bars (Ref. 6) have shown the carrier removal rate under electron irradiation to increase with increasing lithium density, there continue to be questions concerning the role of lithium cells in the formation of damage centers. For this reason, information on the diffusion-length damage constant, K_L, versus lithium gradient was extracted from photovoltaic data (short-circuit current) taken immediately after irradiation. The quantity K_L is defined by

$$\frac{1}{L(o)^2} - \frac{1}{L_o^2} = K_L \phi, \tag{5}$$

where L_o and $L(o)$ are the minority-carrier diffusion lengths in the base region of the cell before irradiation and immediately after irradiation, respectively. Simultaneous short-circuit current and diffusion-length data taken on over 100 lithium cells (see Ref. 2, Figure 2) have resulted in the empirical relation

$$J = 17.0 \log_{10} (L), \tag{6}$$

where J is the short-circuit current density in mA/cm^2 and L is the diffusion length in micrometers. Equations (5) and (6) enable the calculation of K_L for cells whose values of J_o and $J(o)$ are known. The results of such calculations for H3A and C11 solar cells are shown in Figure 3 in which K_L is plotted against dN_L/dw. The curves show a definite dependence on lithium density in both oxygen-rich and oxygen-lean cells indicating that lithium does participate in defects in both types of silicon. It should be noted, however, that no systematic dependence on lithium gradient was found when K_L was based on the post-recovery current, J(R), i.e., when J(R) was substituted for J(o) in Equations (5) and (6). Stated in more practical terms, the value of J(R), in the experiments performed to this date, has been relatively insensitive to dN_L/dw.

E. LITHIUM DENSITY AT EDGE OF DEPLETION REGION

It has been shown above and in previous work that many of the performance parameters of the lithium cell are directly related to the lithium density gradient as calculated from reverse bias capacitance measurements. This has a sound physical basis since the lithium gradient provides a good index of the average lithium density in the base region adjacent to the junction, the region most important to the cell's photovoltaic performance. Over the past two years pre-irradiation lithium density profiles have been obtained on several hundred cells. This data has recently been tabulated in terms of donor density at the

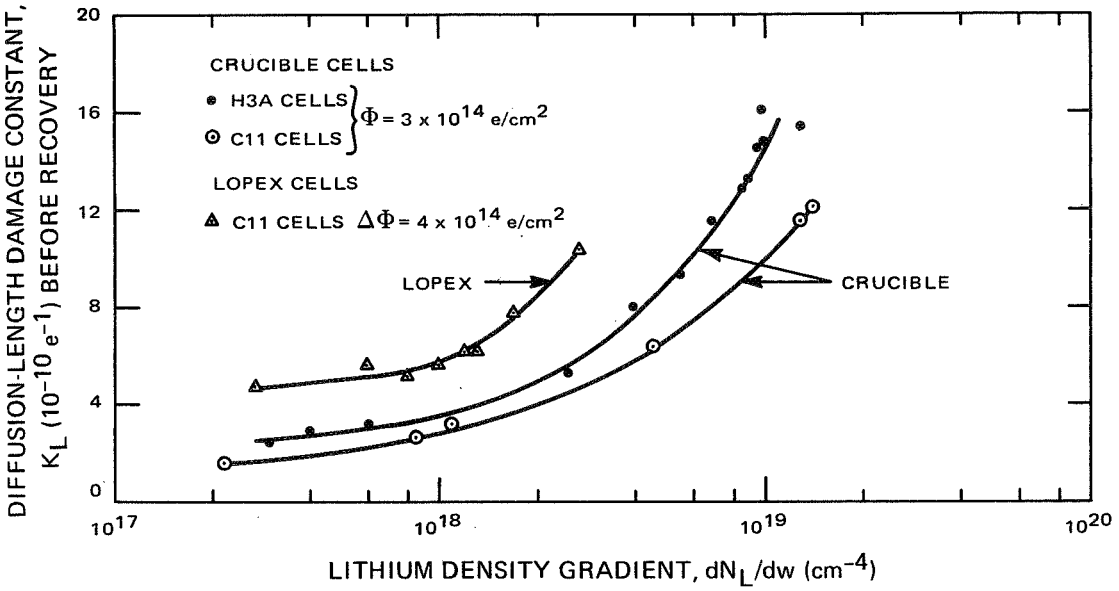

Figure 3. Diffusion-Length Damage Constant (Immediately After Irradiation) vs Lithium Density Gradient for H3A and C11 Cells

edge of the depletion region, N_{DO}, versus lithium density gradient, dN_L/dw. The results for 128 oxygen-lean lithium cells are shown in Figure 4. These indicate that a well defined relationship exists between N_{DO} and dN_L/dw. All but 12 of the cells satisfy the relation

$$N_{DO} = [1250\ (\pm 400)]\left(\frac{dN_L}{dw}\right)^{0.62}, \qquad (7)$$

where the units of N_{DO} and dN_L/dw are cm^{-3} and cm^{-4}, respectively. The twelve cells (circled dots) which fail to satisfy this relation are H1A cells which have light lithium doping and $\approx$ 20 ohm-cm of phosphorus doping making the phosphorus doping at the edge of the depletion region greater than the lithium doping. Thus, all of the oxygen-lean cells in which lithium doping predominates (all cells in which $N_{DO} \approx N_{LO}$) satisfy Equation (7). This correlation exists over a range of lithium gradients from 3×10^{17} to 7×10^{20} cm^{-4}, a factor of over 2000, and includes cells from all three manufacturers (Centralab, Heliotek, and Texas Instruments) with a wide range of lithium introduction (diffusion and redistribution) parameters. It is therefore concluded that this relation is basic to the oxygen-lean lithium cell in the case where $N_{LO} \approx N_{DO}$.

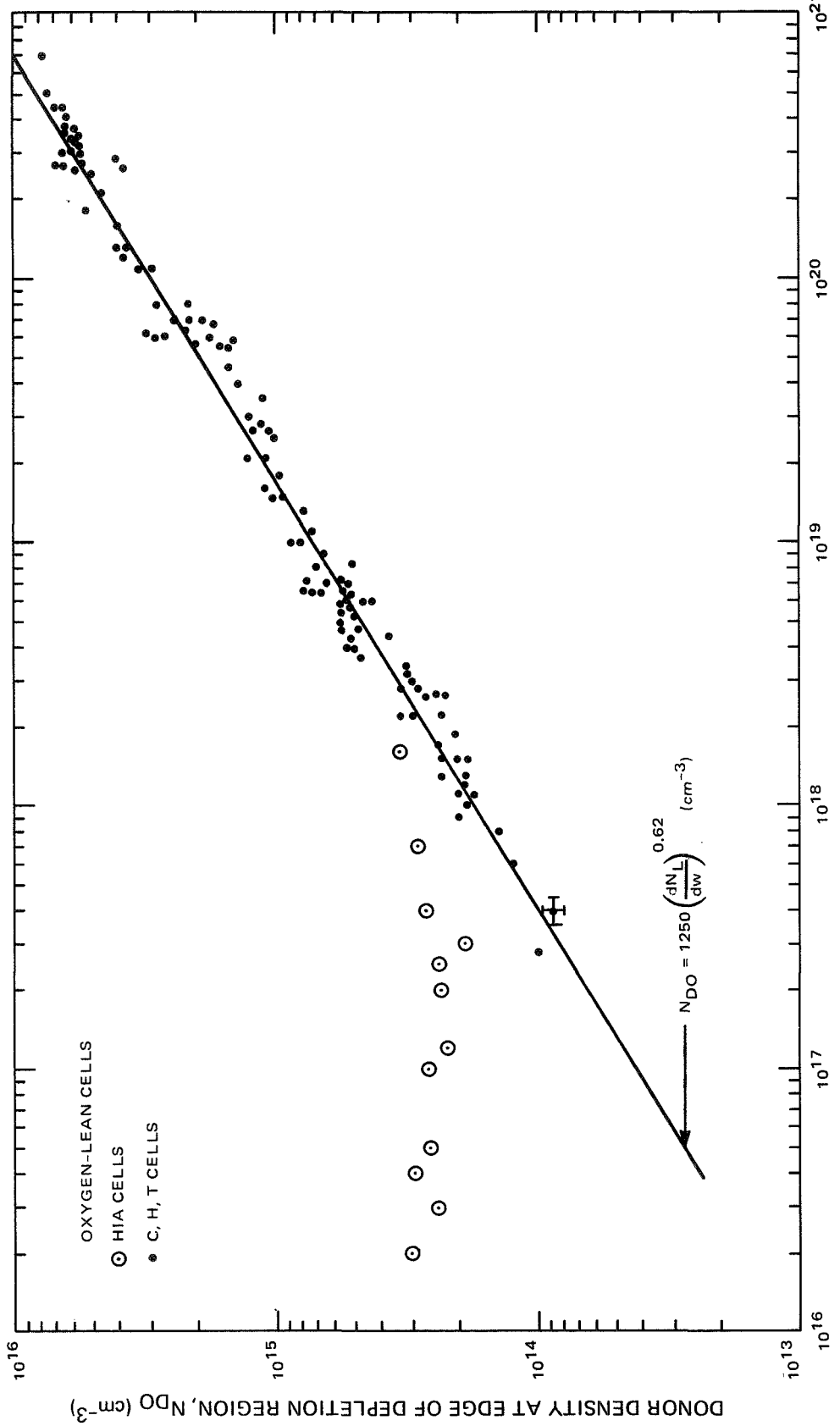

Figure 4. Donor Density at Edge of the Depletion Region vs Lithium Donor Density Gradient — 128 Oxygen-Lean Cells

The physical reasons for this relationship have not yet been uncovered, however the practical consequences are noteworthy. Equation (7) reduces (with a sacrifice in accuracy) the number of capacitance measurements required to predict the recovery speed of lithium cells. To obtain N_{DO} only two capacitance measurements near zero bias are required whereas an accurate determination of dN_L/dw requires capacitance measurements at a minimum of six separate cell biases. Equations (7) and (3) give the recovery speed for oxygen-lean cells in terms of N_{DO};

$$\frac{1}{\theta} \approx \frac{(N_{DO})^{1.6}}{3.1 \times 10^{21}} \tag{8}$$

where θ is in days and N_{DO} is in cm^{-3}. It is felt, however, that the gradient method is more reliable due to the presence of phosphorus or other donors in the base region of the cell.

Similar N_{DO} versus dN_L/dw plots were obtained for seventy oxygen-rich (crucible) cells. The trends were less pronounced due to the higher phosphorus (or arsenic) doping in curcible silicon (starting resistivity $\leqslant 30$ ohm-cm) and the smaller gradient range encompassed by the crucible cells (2×10^{17} to 7×10^{19} cm^{-4}). However, the data, which is plotted in Figure 5, indicates a weaker dependence of N_{DO} on dN_L/dw,

$$N_{DO} \approx 1.1 \times 10^{6} \left(\frac{dN_L}{dw}\right)^{0.46}. \tag{9}$$

Thus the relationship between N_{LO} and dN_L/dw is dependent on oxygen content. This is not surprising in view of the fact that the identity of the lithium donor changes from Li^+ to LiO^+ when the ratio of oxygen concentration to lithium concentration becomes large.

Equations (7) and (9) also enable the calculation of the electric field at the depletion region edge due to the presence of the lithium donor gradient. This field, ϵ, is given by

$$\epsilon = \frac{kT}{eN_{DO}}\left(\frac{dN_L}{dw}\right), \tag{10}$$

where k is Boltzmann's constant, e is the electron charge and T is the cell temperature. In the case of the oxygen-lean cells, combining Equations (7) and (10) yields, at room temperature

$$\epsilon \approx 2 \times 10^{-5} \left(\frac{dN_L}{dw}\right)^{0.38} \text{(V/cm)}. \tag{11}$$

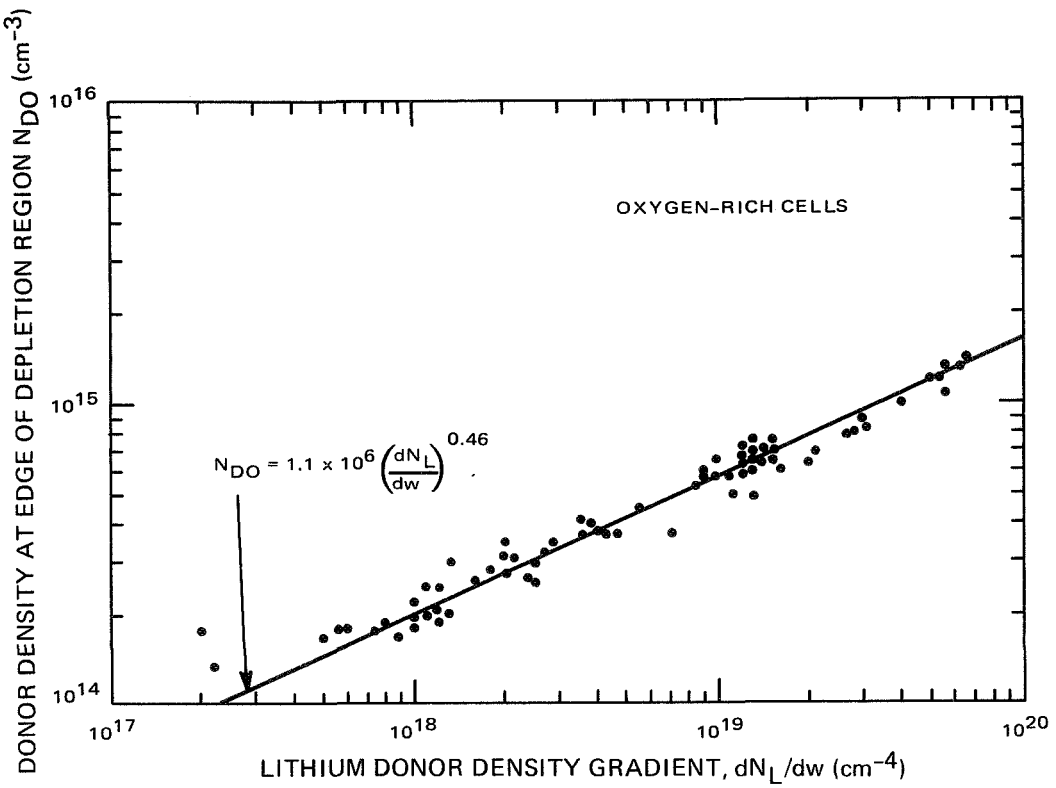

Figure 5. Donor Density at Edge of Depletion Region vs Lithium Donor Density Gradient — 70 Oxygen-Rich Cells

Thus the electric field which can be supported by the lithium gradient at the edge of the depletion region increases with increasing lithium gradient. For example, for $dN_L/dw = 10^{18}$ cm^{-4} the electric field is approximately 150 V/cm as compared with 800 V/cm at $dN_L/dw = 10^{20}$ cm^{-4}. For the higher gradients, the field is probably significant in aiding the flow of minority carriers (holes) toward the junction. A similar situation exists (with stronger gradient dependence) in the oxygen-rich cells.

SECTION III

LITHIUM TRANSPORT AND CELL STABILITY

Due to the high mobility of lithium and the large electric fields near the junction, lithium flow near the junction has a significant influence on lithium cell stability. Capacitance measurements have previously shown that the lithium flows from the base into the depletion region (Ref. 7). The flow rate, Γ, is given by

$$\Gamma = N_L \mu_L \epsilon + D_L \frac{dN_L}{dw}, \tag{12}$$

where μ_L and D_L are the lithium mobility and diffusion constant, respectively; and ϵ is the electric field. In the base, beyond the depletion region,

$$\epsilon_B = \frac{kT}{eN_L} \frac{dN_L}{dw}. \tag{13}$$

Combining Equations (12) and (13) and using the Einstein relation, the lithium flow rate (toward the junction) in the base region Γ_B, is given by

$$\Gamma_B = 2 D_L \frac{dN_L}{dw}. \tag{14}$$

The condition for steady flow is $d\Gamma/dw = 0$.

The great majority of lithium cells tested over the past several years have shown linear density increases (dN_L/dw = constant, or $d^2N_L/dw^2 = 0$) in the base region near the junction. For such cells a steady flow pattern exists (if $dD_L/dw = 0$), giving a stable lithium density distribution near the junction until the lithium reservoir near the back of the cell is depleted. Indeed, most of the lithium cells tested have been stable with respect to open-circuit voltage, which is the principle density-dependent cell parameter. However, a number of C4 cells had shown a loss in open-circuit voltage with time which occurred in both irradiated and unirradiated cells (Ref. 3). The probable reason for this loss is shown in Figure 6 which gives donor density profiles for cell C4-3. The initial profile shows an initial linear rise in donor density; however, beginning at about 0.7 μm the density begins to level off, i.e., d^2N_L/dw^2 becomes negative. This creates a situation in which there is a net lithium flow out of the region ($d\Gamma/dw < 0$) and toward the junction. Consequently, a decrease in donor density occurs (with a corresponding loss in V_{oc}) as illustrated by the density profile in Figure 6 taken 550 days later.

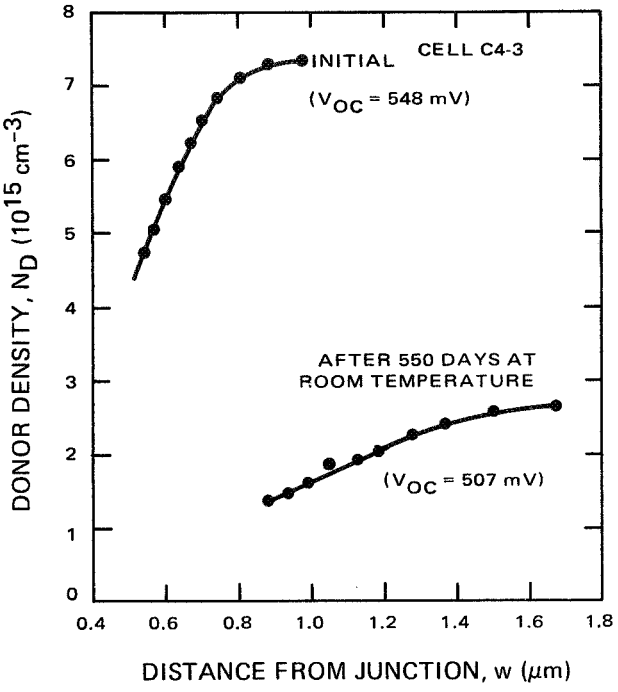

Figure 6. Donor Density vs Distance From Junction Before and After Open-Circuit Voltage Degradation — Cell C4-3

SECTION IV

CONCLUSIONS AND FUTURE WORK

A. CONCLUSIONS

During the present reporting period it has been shown that high performance lithium cells made from both oxygen-rich and oxygen-lean silicon and with a wide range of lithium gradients out-perform commercial 10 ohm-cm n/p cells after recovery from 1-MeV electron fluences up to $3.6 \times 10^{14} e/cm^2$. Under 140 mW/cm^2 tungsten illumination, the post-recovery maximum powers of the lithium cells exceed those of simultaneously irradiated n/p cells by up to 20 percent. The recovered value of open-circuit voltage after fluences in the $3 \times 10^{14} e/cm^2$ range was found to have a strong dependence on the lithium gradient, increasing monotonically with gradient and ranging from 500 to 560 mV over a gradient range from 4×10^{17} to $1.3 \times 10^{19} cm^{-4}$.

As was previously observed in oxygen-lean (C11C) cells, oxygen-rich (C11B) cells were shown to recover at a rate approximately proportional to the lithium density gradient. This established an approximate recovery relation for all lithium cells irradiated to a fluence of $1 \times 10^{14} e/cm^2$, namely

$$\theta D_L dN_L/dw \approx 5 \times 10^8 cm^{-2}.$$

Capacitance measurements on several hundred cells indicate that a unique relationship exists between the lithium gradient and the lithium donor density at the edge of the depletion region. This reduces the number of capacitance measurements required to obtain an approximate value for the lithium gradient. Capacitance measurements have also traced the probable cause for previously reported open-circuit voltage degradation in C4 cells to a levelling off of the lithium density in the base region near the junction.

B. FUTURE PLANS

Recovery and stability tests will continue. Measurements of cell recovery properties versus lithium gradient will be extended to higher fluences and a wider range of gradients will be used where possible. A study of the transport properties of lithium donors in the region near the junction has been initiated.

REFERENCES

1. J. Hilibrand and R. D. Gold, RCA Rev. 21, 245 (1960)
2. T. Faith, G. Brucker, and A. Holmes-Siedle, Fifth Quarterly Report, JPL Contract No. 952555, Prepared by RCA and issued Oct. 10, 1970.
3. T. Faith, J. P. Corra, and A. Holmes-Siedle, Conference Record of the Eighth Photovoltaic Spec. Conf. IEEE Catalog No. 70C 32 ED, 247 (1970).
4. G. Brucker, T. Faith, J. P. Corra, and A. Holmes-Siedle, Fourth Quarterly Report, JPL Contract No. 952555, Prepared by RCA and issued July 10, 1970.
5. E. M. Pell, Phys, Rev. 119, 1222 (1960), J. Appl. Phys. 32, 6 (1961).
6. G. Brucker, Phys, Rev. 183, 712 (1969).
7. T. Faith, G. Brucker, A. Holmes-Siedle, and R. Neadle, IEEE Trans on Nuclear Sci NS-15, 61 (1968).

RCA | Government and Commercial Systems | Astro Electronics Division | Princeton, New Jersey